NUMERICAL INVESTIGATION INTO THE UNSTEADY EFFECTS OF NON-AXISYMMETRIC TURBINE ENDWALL CONTOURING ON SECONDARY FLOWS

Dwain Dunn[1]
Glen Snedden
CSIR

Pretoria, Gauteng,0001
South Africa
Email: [1]ddunn@csir.co.za

Theodor W. von Backström

Department of Mechanical and Mechatronic Engineering
University of Stellenbosch
Private Bag X1, Matieland 7602
South Africa

Abstract

Turbine manufacturers are continually striving to improve turbine performance, and thus reduce emissions, which has been accelerated with the inception of the Kyoto protocol. One of the areas that have received attention is the controlling of secondary flows. The current investigation looks at the use of endwall contouring to reduce the effect of secondary flows. Endwall contouring has been shown to have promise by several researchers.

The numerical investigation was based on the experimental geometry which was based on the cascade geometry of Ingram. The same boundary conditions were used, but the numerical investigation was unsteady. The steady state experimental and numerical results were also used as a basis for comparison of the isentropic stage total-to-total efficiency.

The experimental time averaged velocity magnitude plots show reasonable correlation, but fail to capture the steep gradients between 25% and 35% span and between 75% and 85% span.

Looking at the time dependent streamtubes it becomes obvious that there was little if any difference to the secondary flows due to wake propagation. The streamtubes show that the upstream stator wake had a minor effect on the secondary flow; however the downstream stator's stream tubes did show some oscillations. Thus there could be a greater advantage to contouring blade rows downstream to the first rotor; however this remains to be investigated.

It was found that the computed efficiencies of the unsteady and the steady state analysis were different. It is evident that there are no correlations to be seen, the difference appears to be random. Upon inspection it was found that using isentropic efficiency for comparison was not appropriate at such low Mach numbers, due to its sensitivity to errors in temperature and pressure. Snedden *et al.* highlighted this as well.

Nomenclature

CFD	Computational Fluid Dynamics
S	Span (mm)
y^+	Near wall Reynolds Number
h	Isentropic efficiency
p	Pressure (Pa)
T	Temperature (K)
g	Ratio of specific heats

Subscripts:

1	Stator inlet
3	Rotor outlet
T	Total
Stage	From stator inlet to rotor outlet

Introduction

Secondary flows have been shown to exist in turbomachinery, and are typically defined as being off design flows that cause unexplained secondary losses [1]. Secondary flows in a turbine have a detrimental effect on efficiency, which means a higher cost of operation. Rose [2] stated that increasing the efficiency of a turbine by 0.1% equated to a saving of approximately $22 000 a year in 1994 for a Boeing 747. Denton [3] states that one third of the endwall losses can be shown to be due to the entropy generation in the annulus boundary layer in and around the blade row.

Secondary flows become more prevalent in cases where the aspect ratio decreases, or the aerodynamic duty (blade loading) increases [4]. Therefore as turbine engines get smaller and lighter for a given

thrust rating, the stronger secondary flows become. Therefore a reduction in secondary flow leads to an increase in performance of the turbine engine. One of the methods currently being investigated to control secondary flows is endwall contouring.

Ingram [5] performed linear cascade experiments at Durham University using endwall non-axisymmetric contouring and found that contouring can improve efficiency, if designed correctly. Brennan *et al.* [6], Rose *et al.* [7] and Harvey *et al.* [4] experimentally tested endwall contouring using a model test rig and found up to 0.9% improvements in efficiency.

Snedden *et al.* [8] performed experimental investigations aimed at inspecting the performance of a generic endwall as tested by Ingram [5] in a annular rotating environment. The experiments were aimed at investigating the steady effects, and it was found that the generic endwall contouring improved efficiency in the rotating environment as well.

The current investigation is aimed at a numerical investigation of the unsteady effects on the secondary flows. The secondary flow structure will be investigated as well as blade pressure profiles.

Experimental setup

The steady state experimental set-up was described in Snedden *et al.* [9], and Dunn *et al.* [10]. The test rig used was a 1½ stage low speed test turbine which was initially used to investigate tip loss measurements by Kaiser [11]. For this reason the stators have a tip clearance at the casing. The tip clearance was 0.5 mm for both stators and 1mm for the rotor.

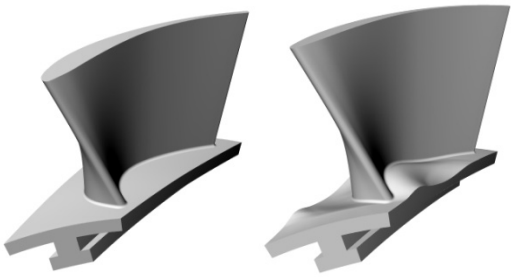

(a) Annular rotor and (b) contoured rotor

Figure 1: Rendered representations of the CSIR rotor blades

The unsteady experimentation was performed using TSI's IFA 300, in conjunction with the Model 1247A-10 cross flow hot film X-probe, calibrated using TSI's Model 1129 auto calibrator. The X-probe only allowed axial and tangential velocity measurements, and thus no radial component was available for comparison/investigation. For each grid point 64 K samples were taken, at a sample frequency of 100 kHz.

The sample grid used consisted of 15 spanwise points and 23 tangential points creating a sample grid consisting of 345 points. The spanwise points were 4 mm apart, and the tangential points were 1˚ apart. The spanwise extent was from r = 145.5 mm to r = 201.5 mm. This equated to a clearance of 2.5 mm between the probe and the endwall, and 1.5 mm between the probe and the casing. Anything smaller could result in damaging the probe. The Rotadata traverse used to move the five-hole probe described in Snedden *et al.* [9] was used to move the X-probe.

Numerical setup

The geometry used is described in Snedden *et al.* [9]. The mesh was described in Snedden *et al.* [8] and Dunn *et al.* [12]. The CAD representation of the blades to be tested can be seen in Figure 1. Figure 2 shows contoured rotor with the mesh on blade and endwalls.

Numeca's FINE^{TM}/Turbo Version 8.3-1 was used for the numerical analysis. The boundary conditions used were the design operating conditions of the turbine test rig used. The boundary conditions are listed in Table 1.

Dunn *et al.* [12] found that the SST k-ω turbulence model predicted the secondary flow features the best out of the available turbulence models in FINE^{TM}/Turbo.

The domain scaling method of FINE^{TM}/Turbo [13] was used to deal with the moving mesh. A requirement of using domain scaling was that the periodicity of the rows must be the same. Due to the number of stator and rotor blades this meant there needed to be three stator blades meshed and two rotor blades, as shown in Figure 2.

A fully structured hexahedral mesh was used that had in excess of 5 million cells. Both of the stators had a 49 cell rows in the radial direction, and the rotor had 81 cell rows. A parabolic distribution was used in the boundary layer regions to increase mesh density,

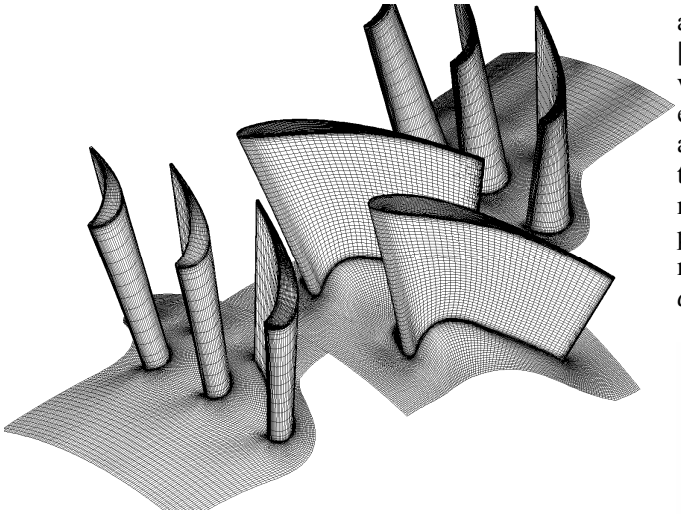

Figure 2: The blades used for the CFD analysis, showing the surface mesh

giving an average $y^+ < 1$ with a maximum of $y^+ = 2.2$ on the blade surface.

Table 1: CFD boundary conditions

Inlet velocity [m/s]	21.38
Inlet temperature [K]	293
Number of rotor blades [-]	20
Number of stator blades [-]	30
Inlet turbulence intensity [%]	< 1
Outlet pressure [kPa]	82.9
Rotational speed [RPM]	2300
Characteristic length [m]	0.06
Characteristic velocity [m/s]	25
Characteristic density [kg/m3]	1.0

Results

A comparison of the experimental and numerical rotor exit velocity magnitude can be found in Figure 3 and Figure 4. With respect to Figure 3, it was evident that the passage vortex intensity was not accurately captured. The spanwise location was also over-predicted by approximately 15% span. The tip leakage flow was not captured well either, with the trend as well as the magnitude being incorrect. The discrepancy was thought to be due to the experimental casing not being perfectly circular in the measurement region. The port used to insert the probe into the flow field was also thought to have a small effect on the flow in the tip region.

Figure 4 shows that for the contoured endwall, the trend was better predicted, except for the retardation in the flow at about 30% span. Tip leakage flow was again poorly predicted, as mentioned in Dunn *et al.* [10]. The correlation from the hub until 20% was very good; the CFD value was with-in the experimental range, with values below 20% span approximating the experimental average values. Due to the under-predicted gradient at 30% span the magnitude at midspan was over predicted. The profile was however replicated reasonably well. For a more detailed experimental analysis refer to Dunn *et al.* [10].

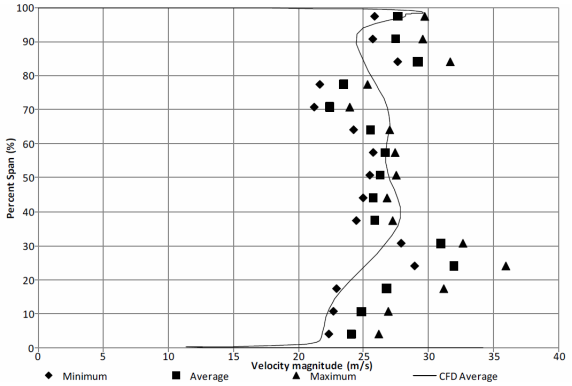

Figure 3: Annular rotor exit velocity magnitude plot

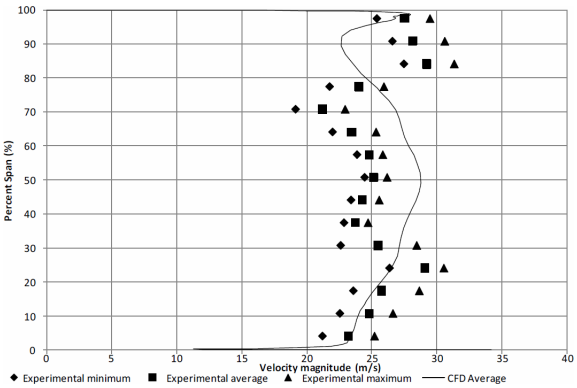

Figure 4: Contoured rotor exit velocity magnitude plot

Figure 5 and Figure 6 show the stream tubes at four different time steps/rotor positions, with the initial position being top left, proceeding clockwise. The four positions shown constitute one rotor blade passing. The stream tubes of both stators were coloured red. For the rotor, the horseshoe vortex streamtubes were coloured red and blue, and the vortex formed by the cross passage endwall flow was coloured green. Stream tubes were released from the same locations as those shown in Snedden *et al.* [8].

The rotor vortex patterns observed were comparable to the steady vortex structure of Snedden *et al.* [8].

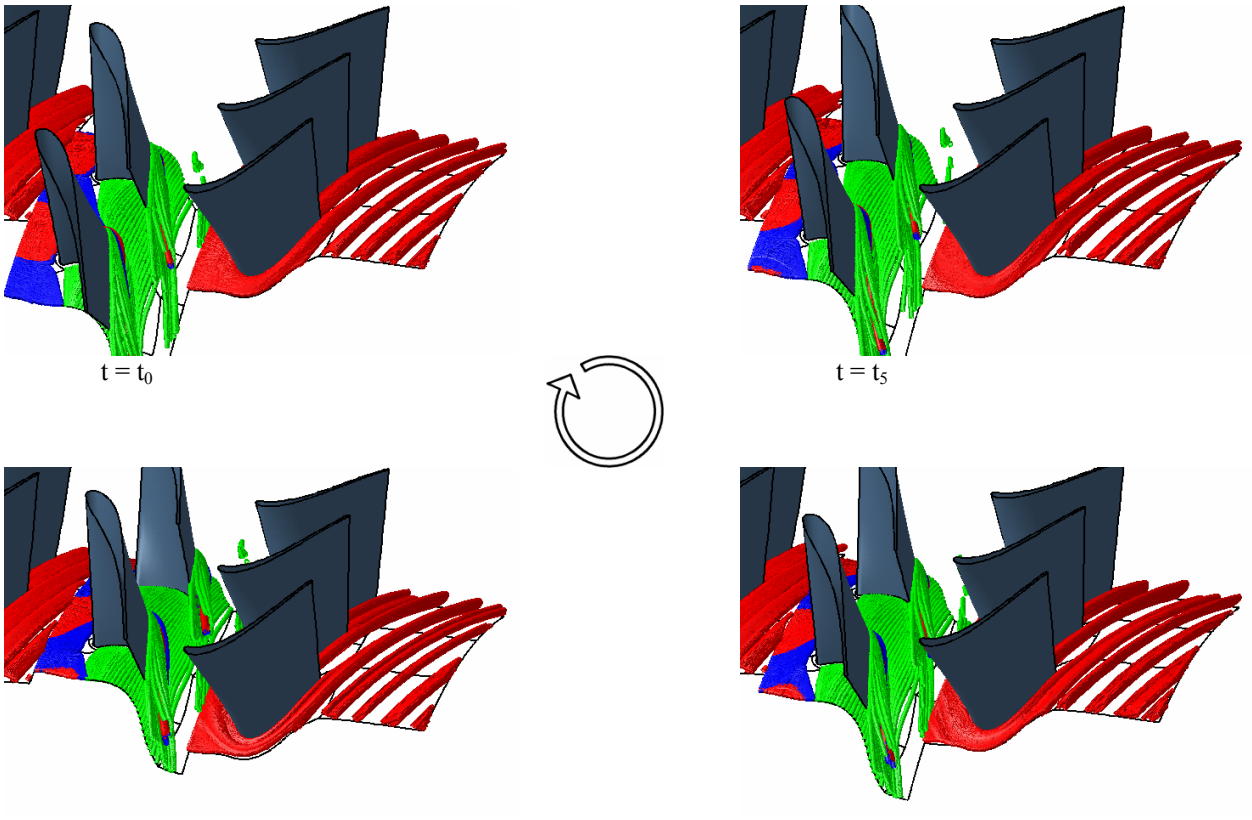

Figure 5: Annular endwall: streamtubes showing secondary flow

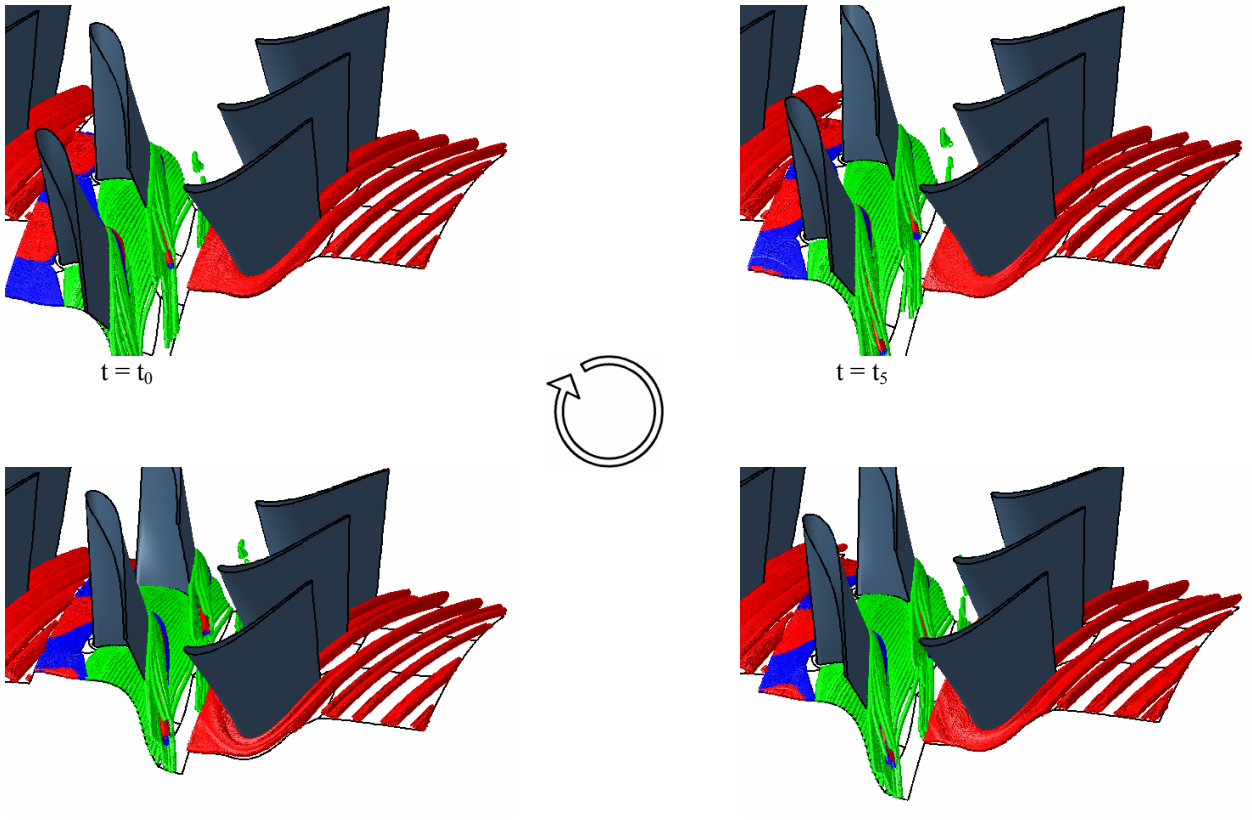

Figure 6: Contoured endwall: streamtubes showing secondary flow

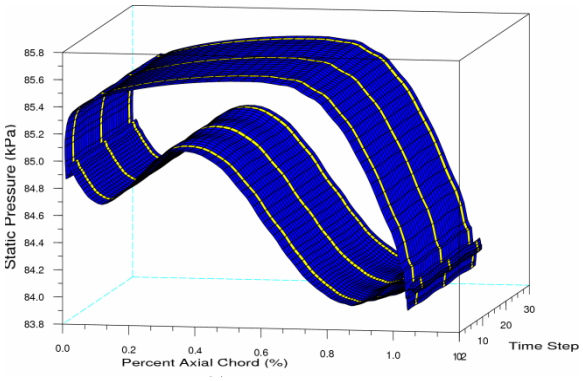

Figure 7: Annular rotor: time varying blade pressure profile plots at 0% span

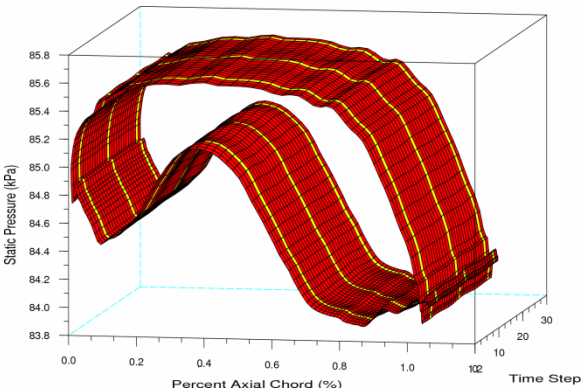

Figure 8: Contoured rotor: time varying blade pressure profile plots at 0% span

The difference between the annular and contoured vortex structures were also the same as reported by Snedden *et al.* [8]. The contoured vortex structure was not as tightly wrapped as that of the annular case. The portion of the passage vortex that originate from the cross passage flow was not as tightly wrapped around the horseshoe vortex in the contoured case as for the annular case, and was spread out more in the spanwise direction.

However it was found that the stream tube location was relatively constant with respect to the rotor blade reference frame. The vortices in the rotor passage were relatively unaffected by the wake of the upstream stator blades.

The blade pressure profiles were investigated in order to determine what effect the wake had on the blade endwall pressure profiles. To facilitate in the visualisation of the fluctuation in time, the pressure plots were done sequentially, creating a surface plot instead of a line plot. The result can be seen in Figure 7 and Figure 8. The yellow bands indicate the location where the wake of the upstream stator was in line with the rotor leading edge, i.e. the location that the wake impinges on the leading edge of the rotor.

It can be seen that there was not much fluctuation in time in the pressure profiles. With regards to the annular case the pressure surface shows negligible variation, where as the suction surface does show some variation, but it was in the order of tens of Pascal's. The contoured case shows slightly more fluctuations on the pressure surface, it is thought that this was due to the contouring of the endwall on the pressure surface being raised. The suction surface shows a similar amount of wake driven oscillation, but the magnitude of which was slightly higher.

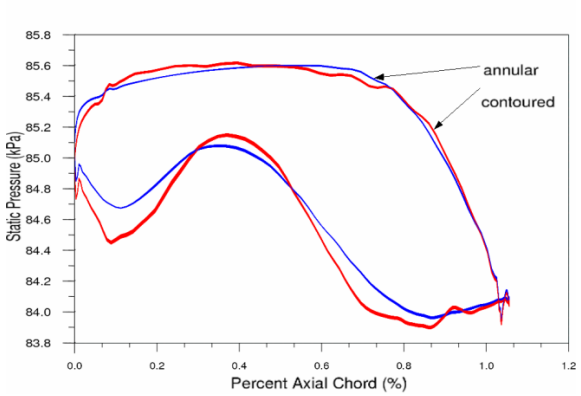

Figure 9: Blade pressure profile plots at 0% span

The combined rotor blade hub pressure profile can be seen in Figure 9, with the contoured profile being red and the annular profile being blue. The time axis was removed and the annular and the contoured profiles plotted together to allow for comparison. The width of the line gives an indication of the amount of fluctuation of the static pressure with respect to time, i.e. the time axis is perpendicular to the page. It can be seen that the contouring reduces the cross passage gradient, and can be described as being more aft loaded then the annular case, as seen in Snedden *et al.* [8]. The loading of the contoured rotor up until 30% was also greater than the annular case, i.e. the rotor blade was front loaded.

The lack of unsteady effects due to the stator wakes was due to the boundary layer keeping the wake effects away from the blade surfaces. Hence the blade static pressure does not fluctuate by a significant amount. Liu and Rodi [14] performed an experimental investigation into wake induced unsteady flow in a linear cascade. It was reported that the integral parameters of the boundary layer were relatively constant with respect to phase, and the values remain close to the time averaged values [14].

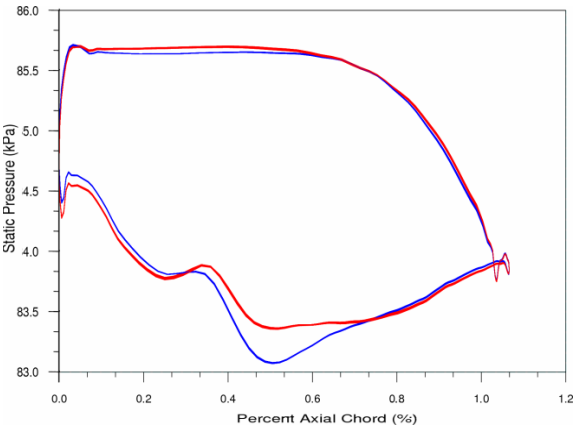

Figure 10: Pressure profile plots at y = 0.17 mm off the blade and 25% span

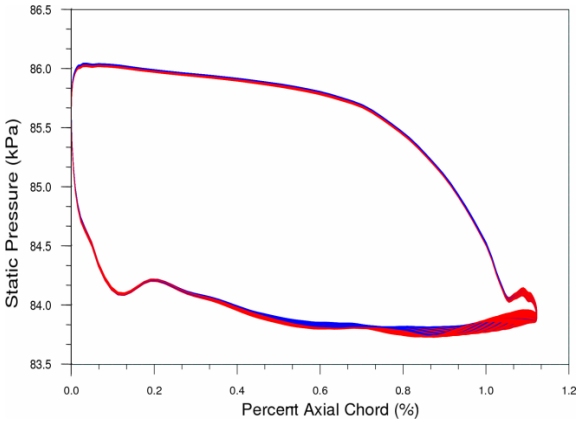

Figure 11: Pressure profile plots at y = 1.15 mm off the blade and 50% span

Pressure profiles at two different distances from the blade were inspected to investigate the dampening effect of the boundary layer. The two distances were y = 0.17 mm and y = 1.15 mm perpendicularly off of the rotor blade, at 25% span, Figure 10 and 50% span, Figure 11. It can be seen that close to the endwall, Figure 10, there are relatively few oscillations. At 50% span however it can be seen that there are large oscillations towards the trailing edge on the suction surface, an observation also made by Lott *et al.* [15]. The pressure profile at y = 0.17 mm and 25% span, Figure 10 was still too close to the blade surface to show any unsteady features. It should be noted however that the contouring has an effect on the pressure profiles at

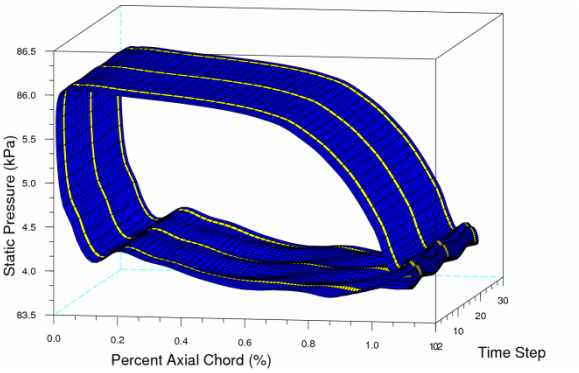

Figure 12: Annular endwall: pressure profile plots at y = 1.15 mm off the blade and 50% span

this distance. The cross passage pressure gradient was reduced for the contoured rotor, and the blade was more front loaded. Knezevici *et al.* [16] state that front-loading of a high lift rotor is advantageous from a midspan performance perspective. It was also stated that front-loading offered good stall characteristics for a wide range of operating conditions.

Isentropic efficiency comparisons

Finally the steady and unsteady stage total-to-total efficiencies were compared. The steady state CFD and experimental stage total-to-total efficiencies were taken from Snedden *et al.* [8]. The unsteady data was time-averaged in order to make the comparison. The stage total–to-total isentropic efficiency was calculated using [17]:

$$\eta_{stage} = \frac{1 - \frac{T_{T3}}{T_{T1}}}{\left(1 - \frac{P_{T3}}{P_{T1}}\right)^{\frac{\gamma-1}{\gamma}}} \qquad (1)$$

Where T_T is the total temperature and P_T is the total pressure. The subscript 1 indicates stator inlet (stage inlet) and 3 indicates rotor exit values. There was no unsteady experimental data since the experiments were performed with hot film probes, thus efficiency cannot be calculated because time

Table 2: Stage total-to-total efficiency comparison

	Annular	Non-axisymmetric	D
Steady experiment	77%	77.4%	0.4%
Steady CFD	86.8%	86.3%	0.5%
Unsteady CFD	86.2%	86.4%	0.2%

dependent temperature and pressure were not available.

Table 2 shows the comparison of total-to-total efficiencies. It was found that the efficiencies were not representative of the steady state experimental results, or the steady state CFD results. The experimental and time-averaged unsteady state total-to-total efficiency difference were both positive, whereas the steady state CFD was negative. In other words the unsteady CFD and steady state experiments predicted that the contouring improved the stage efficiency, whereas the steady CFD predicted that the contouring reduced the stage total-to-total efficiency.

The stage temperature difference (temperature across inlet stator and rotor) in the CFD was approximately $\Delta T = 2.5^{\circ}C$. Upon inspection of Equation 1 it was noted that with such a small temperature difference, any error in the temperature equates to a large efficiency change. An error in temperature of $\Delta T = 0.1\%$ equates to a change in stage total-to-total efficiency of $\eta_{stage}=10.8\%$. If the same error (0.1%) occurs in pressure, the change in stage total-to-total efficiency of $\eta_{stage} = -2.7\%$.

Due to the large change in stage total-to-total efficiency for such a small percentage change in temperature and pressure, it was felt that using stage total-to-total efficiency was a poor choice for comparison. The difference in inlet and outlet density, due to the low pressure (and Low Mach Number) tested, meant that the changes in density start to occur outside of the accuracy of the solver, which was a density based solver. The FINE^{TM}/Turbo does however make use of preconditioning to account for small changes in density.

The typical difference in density used in these tests was less than 4%, and thus should be used with a numerical scheme that has its accuracy much greater then second order. It was noted by Lott *et al.* [15] that isentropic efficiency was not suitable to fully describe turbomachinery performance, since it does not take into account the effect of secondary flows and exit angle effects on blade rows downstream.

Conclusions

It has been shown that non-axisymmetric endwall contouring designed for use in a cascade works in an annular rotating environment. Even though the cascade contouring works, it was felt that a custom contour would improve efficiency further [8].

Viewing of the secondary flow structure revealed that the upstream wakes have very little impact on the size and location of the passage vortex. Boundary layer dampening/deflection was thought to be the reason for this. Small fluctuations from the average value do not have sufficient energy to penetrate the boundary layer. Unsteady fluctuations were found to only start at approximately 2/3 of the axial chord at 50% span and 1.17 mm off the blade surface along the blade, but the oscillations did not penetrate the boundary layer.

It was found that contouring can be used to front load and aft load a turbine blade without changing the blade profile. Front loading reduces profile losses [18] and aft loading reduces secondary flows [19]. Thus not only does the contouring reduce the strength of the passage vortex, it also changes the rotor blade loading profile to one that is more advantageous.

Isentropic efficiency was found to be unsuitable for comparison of the effectiveness of the contoured endwall, especially due to the small changes in temperature and pressure at the low Mach numbers tested. Lott *et al.* [15] found this was also true for high Mach numbers. Secondary kinetic energy and helicity (or a combination of the two) have been proposed by several researchers [8,20,21]. More work into which parameters should be used as an objective function for endwall design and evaluation do however need to be performed.

References

[1] Moore, J., 1985. *"Calculation of 3D flow without numerical mixing"*. AGARD-LS-140 3D Computational Techniques applied to Internal Flows in Propulsion Systems, pp. 8.1–8.15.

[2] Rose, M., 1994. "Non-axisymmetric endwall profiling in the HP NGV's of an axial flow gas turbine". In ASME 94-GT-249, pp. –.

[3] Denton, J., 1993. *"Loss mechanisms in turbomachines"*. In ASME Gas Turbine Congress, Scholars Paper, pp. 1–40.

[4] Harvey, N., Brennan, G., Newman, D., and Rose, M., 2002. "Improving turbine efficiency using non-axisymmetric endwalls: Validation in the multi-row environment and with low aspect ratio blading". In ASME TURBO EXPO 2002, ASME 2002-GT-30337, pp. –.

[5] Ingram, G., 2003. "Endwall profiling for the reduction of secondary flow in turbines". PhD thesis, University of Durham, July.
[6] Brennan, G., Harvey, N., Rose, M., Fomison, N., and Taylor, M., 2001. *"Improving the efficiency of the trent 500 hp turbine using non-axisymmetric end walls: Part 1 turbine design"*. In ASME TURBO EXPO 2001, ASME 2001-GT-0444, pp. –.
[7] Rose, M., Harvey, N., Seaman, P., Newman, D., and Mc-Manus, D., 2001. *"Improving the efficiency of the trent 500 hp turbine using non-axisymmetric end walls: part 2: Experimental validation"*. In ASME TURBO EXPO 2001,ASME 2001-GT-0505, pp. –.
[8] Snedden, G., Dunn, D. I., Ingram, G. L., and Gregory-Smith, D. G., 2009. *"The application of non-axisymmetric endwall contouring in a single stage, rotating turbine"*. In ASME Turbo Expo, no. GT2009-59169.
[9] Snedden, G., Roos, T., Dunn, D., and Gregory-Smith, D., 2007. "Characterisation of a refurbished 1 1/2 stage turbine test rig for flowfield mapping behind blading with nonaxisymmetric contoured endwalls". In ISABE, no. ISABE 2007-1363.
[10] Dunn, D. I., Snedden, G., and von Backström, T., 2009. "Experimental investigation into the unsteady effects of non-axisymmetric turbine endwall contouring". In SACAM2010, SACAM10-079, pp. –.
[11] Kaiser, I., 1996. "The effect of tip clearance and tip gap geometry on the performance of a one and a half stage axial gas turbine". PhD thesis, University of KwaZulu Natal.
[12] Dunn, D. I., Snedden, G., and von Backström, T., 2009. *"Turbulence model comparisons for a low pressure 1.5 stage test turbine"*. In ISABE-2009-1258, pp.–.
[13] Numeca, 2007. User Manual FINE^{TM}/Turbo v8 (including Euranus) Documentation v8a, v8a ed. Numeca International, 5, Avenue Franklin Roosevelt, 1050 Brussels, Belgium, October.
[14] Liu, X., and Rodi, W., 1994. "Velocity measurement of wake-induced unsteady flow in a linear turbine cascade". Experiments in Fluids, 17, pp. 45–58.
[15] Lott, P. T., Hills, N. J., Chew, J. W., Scanlon, T., and Shahrokh, S., 2009. *"High pressure turbine stage endwall profile optimisation for performance and rim seal effectiveness"*. In ASME Turbo Expo 2009: Power for Land Sea and Air, ASME GT2009-59923, pp. –.
[16] Knezevici, D., Sjolander, S., Praisner, T., Allen-Bradley, E., and Grover, E., 2009. "Measurements of secondary losses in a high-lift front-loaded turbine cascade with the implementation of non-axisymmetric endwall contouring". In ASME Turbo Expo 2009: Power for Land Sea and Air, ASME GT2009-59677, pp. –.
[17] Saravanamuttoo, H., Cohen, H., and Rogers, G., 2001. *"Gas Turbine theory"*, 5th ed. Pearson Education Limited.
[18] Howell, R., Ramesh, O., Hodson, H., Harvey, N., and Schulte, V., 2000. *"High lift and aft loaded profiles for low pressure turbines"*. In ASME Turbo Expo 2000 Paper 2000-GT-261, pp. –.
[19] Pullan, G., Denton, J., and Curtis, E., 2005. *"Improving the performance of a turbine with low aspect ratio stators by aft-loading"*. In ASME Turbo Expo 2005: Power for Land Sea and Air, ASME GT2005-68548, pp. –.
[20] Reising, S., and Schiffer, H.-P., 2009. "Non-axisymmetric end wall profiling in transonic compressors. part i: Improving the static pressure recovery at off-design conditions by sequential hub and shroud end wall profiling". In ASME Turbo Expo 2009: Power for Land Sea and Air, ASME GT2009-59133, pp. –.
[21] Reising, S., and Schiffer, H.-P., 2009. "Non-axisymmetric end wall profiling in transonic compressors. part ii: Design study of a transonic compressor rotor using nonaxisymmetric end walls - optimization strategies and performance". In ASME Turbo Expo 2009: Power for Land Sea and Air, ASME GT2009-59134, pp. –.